experimentally convenient temperature range of 4 to 65 K and are not expected to diminish by more than a factor of 3 or 4 at room temperature (*12*).

Characteristics of the spin transistor are appropriate for numerous applications, such as an element in a solid-state nonvolatile memory array (Fig. 4). Here F1 would be composed of a ferromagnet with a relatively large coercivity, and the film would be magnetically biased so that one edge of the hysteresis loop would be near $H = 0$. Film F2 would have a smaller coercivity. An initial, saturating magnetic field would align all of the films. An array of wires fabricated over the elements would write the state of the switch (*14*); the passage of current pulses through write wires w_i and w_j would provide a field pulse of one polarity or another adequate to orient F2 either parallel or antiparallel to F1. The operator could then read the state of the element by closing switches to lines r_i and r_j and sending a current pulse through the switch to ground. A voltage pulse of plus or minus polarity is sent to an amplifier at the end of read line r_j. Because the signal is bipolar, the discriminator can be set to zero, and the pulse is easily amplified. The result would be a solid-state nonvolatile memory, integrated on the same semiconductor chip as the logic elements and able to be accessed with comparable speed. A single element (Fig. 4) can be used as a magnetometer, like the sensing element of a read head for disks and tapes. This single element, in conjunction with a single write wire, also represents a five-terminal embodiment of the spin transistor used as a current, or power, amplifier in which a small, digitally modulated write current modulates a larger read current. The speed of the device is determined by carrier diffusion, spin relaxation, and domain switching times, with the latter imposing a limit of about 10 GHz.

More generalized attributes give reason for optimism about future development. In an analysis that parallels transistors, the spin transistor has a high degree of spin-polarized emission ($\approx$1), a high fraction of spin transmission ($\approx$0.96) and spin collection ($\approx$1), and (on the basis of measurements of spin impedances) a gain of order 1000. The inverse scaling of signal with sample volume bodes well for microfabrication (*15*), although stable domain configurations (such as the "window pane") will be required as film dimensions are reduced. It has been shown that high-quality transition-metal ferromagnet films can be grown on silicon (*16*), so spin-transistor devices could readily be integrated with silicon technology. Spin injection in two-dimensional electron gases has not yet been attempted and offers other possibilities for integrated devices (*17*). If spin injection in semiconductors can be demonstrated, the fourfold multiplicity of carriers would permit the creation of entirely new categories of devices.

REFERENCES AND NOTES

1. M. Johnson and R. H. Silsbee, *Phys. Rev. B* **35**, 4959 (1987); see appendix for the generalized solution.
2. A. G. Aronov, *Sov. Phys. JETP* **24**, L32 (1976) [translation from *Pis'ma Zh. Eksp. Teor. Fiz.* **24**, 37 (1976)].
3. M. Johnson and R. H. Silsbee, *Phys. Rev. Lett.* **55**, 1790 (1985); *Phys. Rev. B* **37**, 5312 (1988); *ibid.*, p. 5326.
4. The longitudinal relaxation time T_1 refers to a change of spin orientation along a direction parallel with an applied field and thus involves a change of energy. The transverse relaxation time T_2 refers to changes of spin orientation that are not accompanied by a change of energy. In the approximation of negligible external fields, we will assume that T_2 is the appropriate parameter.
5. M. Johnson, *Phys. Rev. Lett.* **67**, 3594 (1991).
6. R. H. Silsbee, *Bull. Magn. Resonance* **2**, 284 (1980).
7. J. R. Haynes and W. Shockley, *Phys. Rev.* **75**, 691 (1949).
8. J. Bardeen and W. H. Brattain, *ibid.*, p. 1208; and references therein.
9. R. Meservey, D. Paraskevopoulos, P. M. Tedrow, *Phys. Rev. Lett.* **37**, 858 (1976).
10. The nonlinear characteristic of *pn* junctions results in power gain in the transistor. The FN junctions have not shown nonlinearity, and power gain in the three-terminal embodiment of the spin transistor (for the case where N is Au) is thus unlikely.
11. When F1 and F2 are different materials, the sign convention of the expected effect in Fig. 2B may reverse if η_1 and η_2 have opposite signs.
12. M. Johnson, *Phys. Rev. Lett.*, in press.
13. Commercial SQUID from Biomagnetic Technologies, Inc.
14. A similar technique is used for the manipulation of the magnetization states of magnetoresistive films; see A. V. Pohm, J. S. T. Hwang, J. M. Daughton, D. R. Krahm, V. Mehra, *IEEE Trans. Magn.* **24**, 3117 (1988).
15. Surface states, which impair semiconductor device characteristics as devices are miniaturized, have no analog in spin devices.
16. G. A. Prinz, *Science* **250**, 1092 (1990); R. F. C. Farrow *et al.*, *Mater. Res. Soc. Symp. Proc.* **102**, 483 (1988).
17. S. Datta and B. Das, *Appl. Phys. Lett.* **56**, 665 (1990).

18. I acknowledge a useful conversation with E. Yablonovitch.

5 November 1992; accepted 25 January 1993

Structure of Langmuir-Blodgett Films of Disk-Shaped Molecules Determined by Atomic Force Microscopy

Jack Y. Josefowicz,* Nicholas C. Maliszewskyj, Stefan H. J. Idziak,† Paul A. Heiney,‡ John P. McCauley, Jr.,§ Amos B. Smith III

Monolayer Langmuir-Blodgett films of a discotic mesogen have been studied with atomic force microscopy (AFM). These measurements confirm the "edge on" arrangement for the disk-shaped molecules suggested by surface pressure–area isotherms and show that the molecules form columns that are separated by 17.7 angstroms ± 10 percent. Column alignment is found to be predominantly along the film deposition direction, with an angular spread of 35°. The AFM images also show that the mean disk separation within the columns is 5.1 ± 1.3 angstroms, in good agreement with x-ray diffraction (XRD) results. Room-temperature XRD measurements on bulk samples of the same material indicate a disordered-hexagonal liquid crystalline mesophase, with a column-to-column spacing of 19.9 ± 0.2 angstroms.

Thin films that display anisotropic dc conductivity are of interest both because they are model low-dimensional systems and because of their potential applications. Anisotropy within the plane of the film may be valuable for display applications, whereas films that are highly conductive in the direction normal to the surface could be used as pressure sensors and similar devices (*1*). A promising approach to the preparation of such films is the formation of conductive Langmuir-Blodgett (LB) (*2*) films. Typically, LB films are composed of organic, amphiphilic linear chains. However, disk-shaped molecules exhibiting columnar liquid crystalline mesophases (*3*), which generally have rigid, π-conjugated cores and flexible hydrocarbon substituents, although not manifestly amphiphilic, have under some circumstances been shown to form Langmuir (*4–8*) and LB (*4*, *8*) films. Furthermore, the conductivity of a number of discogenic compounds has also been observed to increase by up to six orders of magnitude after doping by electron acceptors such as iodine (*9*). This conductivity can be highly anisotropic, with most of the conduction occurring along the column axis.

Surface spreading pressure isotherm measurements (*2*) suggest that, depending on their architecture, discogenic mesogens typically exhibit one of two possible orien-

tations when placed at the air-water interface, as indicated schematically in Fig. 1B. In one case the core lies flat on the water surface and the hydrocarbon chains extend away from the interface (*4–6*); we will refer to this as the "face-on" configuration. Such a configuration may be preferred if the core of the molecule is capable of hydrogen bonding, and it also maximizes the configuration space available to the aliphatic tails. In the other case the core sits perpendicular to the interface with two or more chains submerged in the water (*6–8*, *10*); we will refer to this as the "edge-on" configuration. Such a configuration maximizes the π-π interactions between the conjugated cores if the molecules are arranged into columns parallel to the water surface, forming the two-dimensional analog of a columnar phase.

These observations suggest that conductive LB films composed of disk-shaped molecules could be fabricated in either of the configurations discussed above, with the transport characteristics depending on both the molecule selected and the details of the deposition technique. In the edge-on configuration, with the molecules forming columns that lie parallel to the surface, one might expect anisotropic conductivity along one direction in the plane. Conversely, in the face-on configuration, with the molecules lying flat on the surface, a multilayer LB film should be highly conductive in the direction normal to the surface.

To achieve these aims, it is crucial that the details of the microstructure be well characterized, because the conductivity will most likely be limited by defects in the ideal thin film structure. A variety of diffraction and spectroscopic probes have been used to study LB films of discogenic molecules (*4*, *10*), but such techniques are not ideally suited for clarification of the microscopic structure. LB film monolayers have also been studied by scanning tunneling microscopy (*11*), but this technique as well is limited to conductive substrates and layers with thicknesses less than 20 to 30 Å. By contrast, atomic force microscopy (AFM) (*12*) has been used to image structures with atomic resolution for both conductors (*13*) and insulators (*14*), including polymers (*15*) and quite recently LB films (*16*). In this report we present the results of an AFM study of a LB monolayer composed of discogenic molecules. For this film we find that the edge-on configuration is preserved when the film is transferred from the water surface to the solid substrate.

The molecule 6,7,10,11-tetrakis(pentyloxy)-2,3-triphenylenedicarboxylic acid dibutyl ester (**1**) (Fig. 1A) was synthesized by the method of Wenz (*17*) from 3,4-di-*n*-pentoxybenzylaldehyde and di-*n*-butyl acetylenedicarboxylate. Purification by crystallization from ethanol (95%) produced **1** as a waxy solid (melting point 156° to 167°C), possessing ^1H and ^{13}C nuclear magnetic resonance (500 and 125 MHz) spectra as well as high-resolution mass spectra consistent with the assigned structure.

Optical microscopy, differential scanning calorimetry, and x-ray diffraction (XRD) measurements show that this material has a hexagonal-disordered (D_{hd}) liquid crystalline structure at room temperature and converts to an isotropic liquid at 167°C. The D_{hd} structure consists (*3*) of an ordered hexagonal array of columns within which the disks have only short-range, liquid-like order. Powder XRD measurements show a sharp peak corresponding to an intercolumnar spacing of 20.0 Å; measurements on a single-domain strand (*18*) show six such peaks at 60° spacings in the diffraction plane. Both powder and strand XRD measurements also show a broad feature centered around 1.3 $Å^{-1}$ and a somewhat better defined feature at 1.79 $Å^{-1}$. We can definitively assign these features to liquid-like scattering from the aliphatic tails and short-range intracolumnar order, respectively (*18*); the mean spacing between the cores within a column is 3.5 Å, and the intracolumnar correlation length is 5 to 10 Å. Reflection-geometry XRD measurements on an LB film of nominal ten-layer thickness show a sharp peak corresponding to a slightly smaller columnar spacing of 19.8 Å and do not display the 1.79 $Å^{-1}$ feature, indicating a certain degree of preferred orientation with respect to the substrate.

Langmuir and LB films of **1** were prepared as previously described (*6*). The subphase was water purified in a Millipore filtration system. A Lauda FW-1 film balance was used to determine the surface pressure of the film. Figure 1A shows a typical Π-*A* isotherm, measured at 21° ± 3°C with a barrier compression rate of 30 $Å^2$/min. The isotherm displays a low compressibility feature at ~80 $Å^2$ per molecule, rising to 17 mN/m. This relatively small molecular area is consistent with the hypothesis that the molecules lie edge-on to the air-water interface. The substrate used for this study was Si(111), with the native

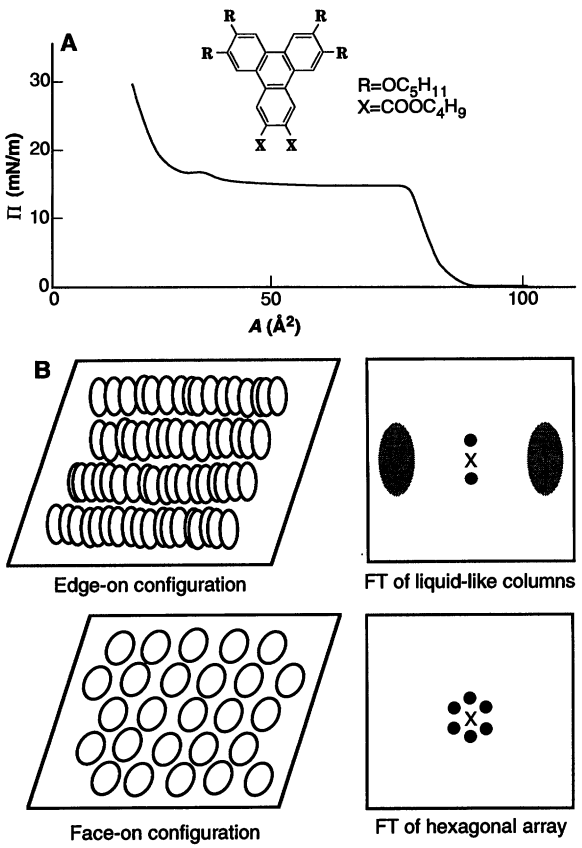

Fig. 1. (**A**) Surface pressure Π versus molecular area *A* isotherm of **1** at room temperature [adapted from (*6*)]. The relatively small area per molecule at the inflection point is consistent with the 80 $Å^2$ per molecule cross-sectional area of a molecule standing edge-on to the surface, but not with the area of a molecule lying flat on the surface. (Inset) Molecular structure of **1**. (**B**) Schematic structure of the edge-on and face-on configurations and their corresponding Fourier transforms. The FT of the edge-on, columnar structure shows sharp peaks corresponding to the inverse of the intercolumnar spacing, oriented along the direction normal to the columns, as well as possibly diffuse maxima attributable to the intracolumnar short-range order. The FT of the face-on, hexagonal structure would show a two-dimensional array of sharp spots.

J. Y. Josefowicz, Materials Science and Engineering Department and Laboratory for Research on the Structure of Matter, University of Pennsylvania, Philadelphia, PA 19104.
N. C. Maliszewskyj, S. H. J. Idziak, P. A. Heiney, Physics Department and Laboratory for Research on the Structure of Matter, University of Pennsylvania, Philadelphia, PA 19104.
J. P. McCauley, Jr., and A. B. Smith III, Chemistry Department and Laboratory for Research on the Structure of Matter, University of Pennsylvania, Philadelphia, PA 19104.

*Visiting Professor from Hughes Research Laboratories, Malibu, CA 90265.
†Present address: Materials Department and Materials Research Laboratory, University of California, Santa Barbara, CA 93106.
‡To whom correspondence should be addressed.
§Present address: Neose Pharmaceuticals, Inc., 102 Witmer Road, Horsham, PA 19104.

oxide layer treated with hexadecyltrichlorosilane (HDTCS) to form a self-assembled monolayer with a hydrophobic surface (*19*). To form the LB monolayer, we dipped the substrate downward through a surface film of 1 held at a constant pressure of 12.5 mN/m. The water surface was then cleaned and the substrate retracted. The ratio of transferred film surface area to covered substrate area was close to unity.

Films were stored in an Ar atmosphere after being transferred and were then imaged ~24 hours later. Images of the film surface were obtained with a Nanoscope III AFM (*20*) at 21°C, with a 1 μm by 1 μm piezoelectric substrate translator having lateral and vertical resolution of less than 0.5 Å. The imaging experiments were carried out with a constant force applied between a microfabricated silicon nitride cantilever tip (*20*) and the LB film surface. Typical applied forces were on the order of 10 nN. The AFM image shown in Fig. 2A is representative of the sample surface in that similar images were obtained over different areas of the sample surface. Images were also found to be stable over the course of 5 hours of repeated scanning and did not change when scanning angles were varied over a range of angles between 0° and 90°. Between the two extreme scanning angles the scanning tip is dragged parallel and perpendicular to the cantilever length direction.

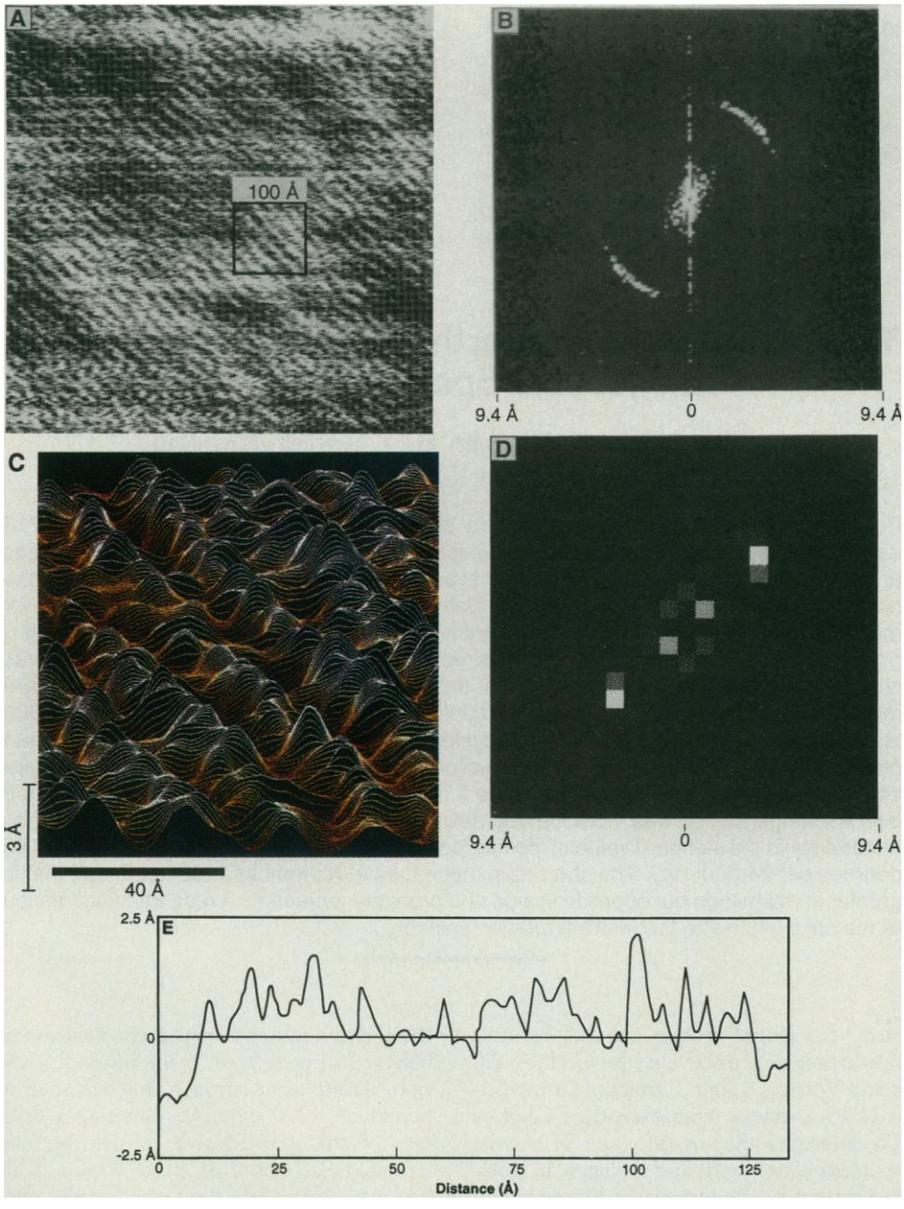

Fig. 2. AFM images of an LB monolayer of **1** on alkylated Si(111). These images have not been filtered or otherwise enhanced. (**A**) Typical AFM image. Note the characteristic columns, which are approximately 18 Å wide, and the presence of local regions with well-defined order, separated by defect regions. The dipping direction for the LB film was approximately parallel to the average column direction. (**B**) Fourier transform (FT) of the image shown in (A). The brightness of the spots is proportional to the absolute value of the FT amplitude. The full scale is 1/9.4 Å, as indicated by the abscissa marks. Note the bright spots situated on an arc corresponding to an intercolumnar distance of 17.7 Å. No other features are seen at smaller interatomic *d* spacings. (**C**) Three-dimensional plot of the boxed region in (A). Within this well-ordered domain, all the columns are essentially parallel and oriented ~45° from the vertical. There is also short-range structure within each column. (**D**) FT of the boxed region in (A). Owing to the high degree of orientational order within this region, only two bright spots are seen. (**E**) Height profiles along the center column in (C).

An AFM image of a single LB film layer of **1** deposited on HDTCS-coated Si is shown in Fig. 2A. This image clearly shows that there is a columnar structure, with the columns oriented predominantly in the direction of deposition of the film. This AFM image indicates that this LB film has the edge-on columnar structure and suggests that the edge-on structure inferred from Π-A studies of the Langmuir film is maintained through the transfer process from the gas-water interface to the coated Si substrate. No evidence of a face-on configuration was found in any AFM images; such a configuration would have led to a close-packed hexagonal or centered rectangular structure. Figure 2B shows the Fourier transform (FT) of the image in Fig. 2A; the brightness of the pixels is proportional to the absolute value of the FT amplitude. Note the resemblance of this FT to the schematic FT shown for liquid-like columns in Fig. 1B. The columnar repeat unit calculated from this FT is 17.7 Å ± 10%. This spacing is slightly smaller than the 19.9 ± 0.2 Å determined from bulk XRD measurements, although at this point the difference is within the error bars of the measurement. We have not yet established whether the first few layers of the film have a smaller columnar spacing; such a difference could result from a perturbation of the structure by the substrate-air interface. In a monolayer molecular film the hydrocarbon tails can point up and away from the interface, allowing the disks to move closer together than they would be in the bulk liquid crystal.

The image in Fig. 2A shows that there are well-defined domains of a single columnar orientation that extend over ~100 Å. These domains are separated by defects that resemble crystal grain boundaries, and the orientations in different domains are slightly different. The FT in Fig. 2B shows that the columns have a spread in orientations of ~35° about the deposition direction. One ordered microdomain has been framed off in Fig. 2A. A three-dimensional AFM image of the region within the frame is shown in Fig.

2C. The image shows columns with a well-defined spacing and a single orientation. This is verified by the FT of the image (Fig. 2D), in which only a single reflection (and its inverse) are evident, corresponding to the repeat units for the columnar separation.

Another feature of our AFM images (see Fig. 2C) is the appearance of maxima along the tops of the columns, which have a characteristic spacing but which are not correlated in position from column to column. This feature is not manifested in the FT images for two reasons. First, the short range of the intracolumnar order should convert sharp peaks in the FT into radial streaks. Second, the lack of intercolumnar correlations (that is, the lack of column-to-column registry of the disks) should further broaden these streaks into weak diffuse maxima. Both types of broadening have been seen in XRD studies of oriented strands of discotic liquid crystals (*18*); the sharp peak corresponding to the intercolumnar spacing is typically two to three orders of magnitude more intense than the diffuse peak corresponding to short-range intracolumnar order. In principle, therefore, the intracolumnar order would be visible as a diffuse feature in the FT of an AFM image with several more decades of dynamic range.

The details of the intracolumnar structure can be seen more clearly in Fig. 2E, which shows the surface profile for a cross section along the top of the column located in the center of the AFM image from Fig. 2C. A statistical analysis of the peak separations (*21*) along all the columns in Fig. 2C shows an average separation of 5.14 Å with a standard deviation of 1.29 Å. If, as suggested earlier, the flexible hydrocarbon tails point up and away from the interface, the AFM tip would tend to interact with them during scanning. However, even with some spread of orientations of the tails, which may be due both to the tip interactions and to the thermally induced motions of the tails, the AFM images show that intracolumnar spacing of the disks ranges from 3.85 to 6.43 Å, in good qualitative agreement with the results of bulk XRD studies presented above.

The observed orientational ordering of this system containing strongly interacting π-conjugated systems suggests its potential for electronic and optical device applications. The clarity that AFM brings to the characterization of these LB films will be valuable in efforts to produce the defect-free, highly oriented films that are essential for such applications.

REFERENCES AND NOTES

1. S. Jin, T. H. Tiefel, R. Wolfe, R. C. Sherwood, J. J. Mottine, Jr., *Science* **255**, 446 (1992).
2. A. Ulman, *Introduction to Ultrathin Organic Films* (Academic Press, Boston, 1991).
3. S. Chandrasekhar and G. S. Ranganath, *Rep. Prog. Phys.* **53**, 57 (1990).
4. D. W. Kalina and S. W. Crane, *Thin Solid Films* **134**, 109 (1985).
5. C. Mertesdorf and H. Ringsdorf, *Liq. Cryst.* **5**, 1757 (1989).
6. N. C. Maliszewskyj *et al.*, *J. Phys. II (France)* **2**, 75 (1992).
7. O. Albrecht *et al.*, *Colloid Polym. Sci.* **264**, 659 (1986).
8. O. Karthaus *et al.*, *Langmuir* **8**, 2279 (1992).
9. L. Y. Chiang *et al.*, *Mol. Cryst. Liq. Cryst.* **125**, 279 (1985); G. B. M. Vaughan *et al.*, *Phys. Rev. B* **46**, 2787 (1992).
10. E. Orthmann and G. Wegner, *Angew. Chem.* **98**, 1114 (1986).
11. D. P. E. Smith *et al.*, *Proc. Natl. Acad. Sci. U.S.A.* **84**, 969 (1987); J. P. Rabe and S. Buchholz, *Phys. Rev. Lett.* **66**, 2096 (1991).
12. G. Binning *et al.*, *Phys. Rev. Lett.* **56**, 930 (1986).
13. G. Binning *et al.*, *Europhys. Lett.* **3**, 1281 (1987); T. R. Albrecht and C. F. Quate, *J. Vac. Sci. Technol. A* **6**, 271 (1988).
14. T. R. Albrecht and C. F. Quate, *J. Appl. Phys.* **62**, 2599 (1987); S. Alexander *et al.*, *ibid.* **65**, 164 (1989).
15. T. R. Albrecht *et al.*, *ibid.* **64**, 1178 (1988).
16. H. G. Hansma *et al.*, *Langmuir* **7**, 1051 (1991); E. Meyer *et al.*, *Nature* **349**, 398 (1991); D. K. Schwartz, G. Garnaes, R. Viswanathan, J. A. N. Zasadzinski, *Science* **257**, 508 (1992); C. J. Eckhardt *et al.*, *Langmuir* **8**, 2591 (1992).
17. G. Wenz, *Makromol. Chem. Rapid Commun.* **6**, 577 (1985).
18. E. Fontes *et al.*, *Phys. Rev. A* **37**, 1329 (1988).
19. J. Sagiv, *J. Am. Chem. Soc.* **102**, 92 (1980).
20. Obtained from Digital Instruments, Santa Barbara, CA.
21. For this analysis, any maximum in the linear trace of a surface profile was taken to be a peak. The average separations and standard deviation were quite insensitive to the method of peak identification.

22. We thank G. Farrington, R. Reynolds, and A. Chester for support. We also thank J. K. Blasie for the use of his Langmuir trough. Financial support was provided by National Science Foundation grants DMR MRL 92-20668 and DMR 89-01219.

14 October 1992; accepted 13 January 1993

The Drift of Saturn's North Polar Spot Observed by the Hubble Space Telescope

John Caldwell, Xin-Min Hua, Benoit Turgeon, James A. Westphal, Christopher D. Barnet

Polar projections of 50 images of Saturn at 889 nanometers and 25 images at 718 nanometers taken by the Hubble Space Telescope in November 1990, as well as 3 images at each wavelength taken in June 1991, have been examined. Among them, 31 show the north polar spot, which is associated with Saturn's polar hexagon, in locations suitable for measurement. In each image, planetocentric coordinates of the polar spot were determined, and the movement of the spot with respect to Saturn's system III rotation rate was studied. During the period of observation, the polar spot had first a short-term westward movement and then a long-term eastward drift. The rate of the long-term drift was −0.060 ± 0.008 degrees per day with respect to system III, approximately 50 percent greater than previously determined from Voyager. The original 1980 and 1981 Voyager data were combined with the new Hubble images to form an 11-year base line. The eastward drift over the longer period was −0.0569 degrees per day. The long-term drift could be due to uncertainty in the standard value of the internal rotation period, which is 810.7939 ± 0.148 degrees per 24-hour day. The short-term movement in November 1990 has a rate that is greater in magnitude but opposite in sign and probably represents a real, transient motion of the spot relative to the internal rotation system.

The hexagonal feature around Saturn's north pole was discovered by Godfrey (*1*) using Voyager 1 and 2 images. To investigate its dynamic characteristics, Godfrey (*2*) measured the rotation rate of a large spot associated with the hexagon in polar projections of the images. In his study and this study, the longitude system is defined by the system III rotation rate (*3*), which is the rotation rate of the magnetic field and is believed to be related to the internal rotation. From seven images that spanned a period of ~270 days, he obtained a drift rate of the spot relative to the internal period, $(-8.13 \pm 0.6) \times 10^{-9}$ rad s^{-1}. It was not clear at the time whether the rate difference represented a real drift of the spot or inaccuracy in the standard value of the internal rotation rate. The existence of the hexagonal feature and the associated polar spot in 50 Hubble Space Telescope (HST) near-infrared images a decade later shows that these features are a persistent phenomenon on Saturn. The larger HST database enables us to make more precise measurements of the movement of these features.

We examined 31 images of Saturn, span-

J. Caldwell and B. Turgeon, Space Astrophysics Laboratory, Institute for Space and Terrestrial Science, and Department of Physics and Astronomy, York University, North York, Ontario, Canada M3J 1P3.
X.-M. Hua and C. D. Barnet, Space Astrophysics Laboratory, Institute for Space and Terrestrial Science, North York, Ontario, Canada M3J 3K1.
J. A. Westphal, Division of Geological and Planetary Sciences, California Institute of Technology, Pasadena, CA 91125.